Author Manuscript

Author Manuscript

Author Manuscript

Author Manuscript

HHS Public Access

Author manuscript

Cell Rep. Author manuscript; available in PMC 2017 October 18.

Published in final edited form as:

Cell Rep. 2017 June 20; 19(12): 2572–2585. doi:10.1016/j.celrep.2017.05.079.

Transduction of repetitive mechanical stimuli by Piezo1 and Piezo2 ion channels

Amanda H. Lewis[1], **Alisa F. Cui**[1], **Malcolm F. McDonald**[1], and **Jörg Grandl**[1,*]

[1]Department of Neurobiology, Duke University Medical Center, Durham, NC 27710, USA

Summary

Several cell types experience repetitive mechanical stimuli, including vein endothelial cells during pulsating blood flow, inner ear hair cells upon sound exposure, and skin cells and their innervating DRG neurons when sweeping across a textured surface or touching a vibrating object. While mechanosensitive Piezo ion channels have been clearly implicated in sensing static touch, their roles in transducing repetitive stimulations are less clear. Here, we perform electrophysiological recordings of heterologously expressed mouse Piezo1 and Piezo2 responding to repetitive mechanical stimulations. We find that both channels function as pronounced frequency filters whose transduction efficiencies vary with stimulus frequency, waveform, and duration. We then use numerical simulations and human disease-related point mutations to demonstrate that channel inactivation is the molecular mechanism underlying frequency filtering, and further show that frequency filtering is conserved in rapidly-adapting mouse DRG neurons. Our results give insight into the potential contributions of Piezos in transducing repetitive mechanical stimuli.

Graphical abstract

[*]Lead Contact and Correspondence: grandl@neuro.duke.edu.

Publisher's Disclaimer: This is a PDF file of an unedited manuscript that has been accepted for publication. As a service to our customers we are providing this early version of the manuscript. The manuscript will undergo copyediting, typesetting, and review of the resulting proof before it is published in its final citable form. Please note that during the production process errors may be discovered which could affect the content, and all legal disclaimers that apply to the journal pertain.

Author Contributions

A.H.L, A.F.C., and M.F.M performed experiments and analyzed data. A.H.L. and J.G. designed the study and wrote the manuscript.

Author Manuscript Author Manuscript Author Manuscript Author Manuscript

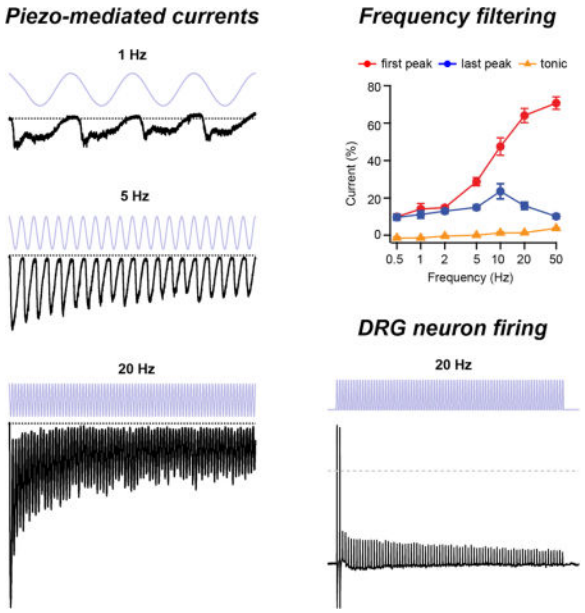

Keywords

Mechanotransduction; Piezo1; Piezo2; mechanosensitive ion channel; repetitive stimulation; frequency filtering; inactivation; three-state gating mechanism; dorsal root ganglia neurons

Introduction

Biological entities process mechanical inputs at several levels, all of which contribute to the phenomenon of mechanotransduction: i) mechanical properties of the tissue determine the extent to which forces cause deformation (Loewenstein and Skalak, 1966; Morley et al., 2016; Qi et al., 2015; Zimmerman et al., 2014); ii) location, numbers, and intrinsic properties of mechanotransducers determine how mechanical force is converted into electrochemical signals (Hao and Delmas, 2010; Hao et al., 2013a); and iii) mechanically insensitive mechanisms influence further signal integration and propagation (Coste et al., 2007; Heidenreich et al., 2011). The encoding of specific features of a repetitive mechanical stimulus, including frequency, amplitude, duration, and phase, likely involves all of these mechanisms. For example, in touch receptors of *C. elegans*, mechanical properties of the tissue attenuate responses of mechanoelectrical transduction channels to sinusoidal frequencies <3 Hz, (Eastwood et al., 2015), whereas in mammals, the location of mechanosensitive hair cells in the cochlea and the mechanical structure of the basilar membrane generate frequency tuning (Robles and Ruggero, 2001). Less is known, however, about the direct contribution of the mechanoreceptors themselves to filtering repetitive stimuli, in part owing to the fact that for many years, their molecular identities in vertebrates remained unknown (Ranade et al., 2015).

Piezo proteins have recently been characterized as the pore-forming subunits of non-selective cationic mechanosensitive ion channels whose expression is required for many mechanotransduction processes (Wu et al., 2016b). The two mammalian isoforms, Piezo1

Author Manuscript Author Manuscript Author Manuscript Author Manuscript

and Piezo2, sense a wide range of mechanical stimuli throughout the body, including various repetitive stimuli (Coste et al., 2010; Coste et al., 2012; Hung et al., 2016; Nonomura et al., 2017; Pathak et al., 2014; Woo et al., 2015). For example, in mice, knockout of Piezo1 results in deficiencies in shear stress-induced vasodilation, whereas knockout of Piezo2 leads to a loss of aversion towards the onset of mechanical vibrations (Ranade et al., 2014a; Ranade et al., 2014b; Wang et al., 2016); likewise, in humans, a loss-of-function mutation in Piezo2 leads to a profound deficit in the ability to detect vibrations of a tuning fork (Chesler et al., 2016).

When exposed to a step-like mechanical stimulus, Piezos activate (open) rapidly in a dose-dependent manner, and subsequently inactivate (entering a non-conducting state) within tens of milliseconds (Coste et al., 2010). Although the molecular mechanism of inactivation remains unclear, it can be modulated by local changes in pH, divalent ion concentration, resting membrane tension, transmembrane voltage, and activity of G protein-coupled pathways (Bae et al., 2015; Dubin et al., 2012; Gottlieb et al., 2012; Jia et al., 2013; Lewis and Grandl, 2015).

Importantly, inactivation is also a key locus for channelopathies. Gain-of-function mutations in Piezo1 and Piezo2 that destabilize inactivation are associated with hereditary xerocytosis and a family of distal arthrogryposis disorders, respectively (Albuisson et al., 2013; Bae et al., 2013a; Coste et al., 2013; Zarychanski et al., 2012).

While isolated, step-like stimulations have been instrumental for measuring overall mechanical sensitivity and characterizing inactivation kinetics of Piezo ion channels in normal and pathological conditions, the mechanical inputs experienced by Piezos *in vivo* are arguably more complex and repetitive in nature. We hypothesized that owing to inactivation, Piezos are not ideal linear transducers of repetitive mechanical stimulations, but rather function as frequency filters, preferentially transmitting salient stimulus information only in a relatively narrow frequency range.

Here, we measure electrophysiologically and simulate numerically how Piezo ion channels in heterologous expression systems and in sensory DRG neurons transduce repetitive mechanical stimuli. We find that Piezos can act as high-pass, low-pass, or bandpass filters, depending on the stimulus waveform and duration, via a mechanism requiring intact channel inactivation. Together, our results characterize Piezos as important components in processing complex mechanical inputs, such as vibrations and blood flow, and identify inactivation as a plastic mechanism for modulating the transduction of these stimuli.

Results

Piezo1 ion channels transduce periodic stimulations with pronounced frequency filtering

To evaluate how Piezo ion channels respond to repetitive stimuli, such as that experienced by a fingertip sweeping over a rough surface (Figure 1A), we transiently expressed mouse Piezo1 in HEK293t cells and recorded inward currents (at −80 mV) in a cell-attached patch clamp configuration, evoked upon periodic pressure stimulation to the patch (Figure 1B). Specifically, we designed a protocol in which a four second sinusoidal test pulse oscillated

Author Manuscript Author Manuscript Author Manuscript Author Manuscript

between +5 mmHg, a pressure we previously demonstrated to minimize membrane curvature, resting membrane tension and Piezo1 open probability by allowing Piezo1 channels to recover from inactivation, and −50 mmHg, a pressure driving open probability to near saturation, while minimizing stress on the membrane patch as well as membrane creep (Figure 1C) (Lewis and Grandl, 2015; Nakayama et al., 2016). Each test pulse was framed between two 300 ms standard step pulses ('$step_1$' and '$step_2$'), which were used to assess initial current density, monitor patch integrity, and quantify channel rundown (Figure S1). In order to minimize potential effects of rundown upon repetitive stimulation owing to long-term inactivation, adaptation or patch deterioration, we only executed one stimulus protocol per patch (Bae et al., 2013a; Gottlieb et al., 2012).

We first tested sinusoidal stimulation at frequencies of 0.5, 1, 2, 5, 10, 20, and 50 Hz, the latter approaching the upper speed limit of our pressure clamp system. All frequencies consistently evoked oscillating inward currents that were apparently phase-locked to the pressure stimulus, with distinct current peaks clearly detectable even at the lowest and highest stimulation frequencies of 0.5 and 50 Hz, respectively (Figure 1C, insets; N = 96 recorded patches). Indeed, Fast-Fourier Transformation (FFT) of the current signal revealed a periodicity matching that of the respective stimulation frequency, and cross correlation analysis revealed a frequency-dependent phase shift (Figure 1D–F). Most strikingly however, the overall profile of the currents varied dramatically with stimulus frequency and duration. Higher frequencies (20 and 50 Hz) elicited large initial peak currents, similar in amplitude to '$step_1$', after which the amplitude of each successive peak decayed over the course of four seconds. In contrast, lower stimulation frequencies (0.5 and 1 Hz) elicited peak currents that were small compared to '$step_1$', and whose amplitudes showed little change throughout the four second stimulation.

Importantly, in recordings from vector-transfected (pcDNA) HEK293t cells, currents were nearly absent at all stimulation frequencies (N = 42), ruling out the possibility that this unusual stimulation protocol activated currents that did not depend on Piezo1 (Figure S2A–D). While HEK293t cells endogenously express small levels of Piezo1 (Dubin et al., 2017; Lukacs et al., 2015), we only analyzed cells with >50 pA peak currents, such that any contribution of endogenous currents to the large currents we observed in an overexpression system would be minimal. Moreover, single channel amplitudes measured during the last second of a 50 Hz stimulation in patches with few channels were identical (35.5±1.7 pS; N = 3) to previously published values for Piezo1 (29–37 pS) (Figure S3A–B) (Coste et al., 2012; Gottlieb et al., 2012; Wu et al., 2016a). Together, these results show qualitatively that Piezo1 ion channels transduce sinusoidal stimuli in a complex manner that depends highly on the stimulus frequency and duration.

In order to obtain a quantitative description and ultimately a mechanistic understanding underlying these currents, we next selected cells meeting specific quality criteria based on responses elicited by '*step1*' and '*step2*'. These included the presence of typical inactivation kinetics and the maintenance of patch integrity following the repetitive stimulus (Figure S1; see Methods for details). This data set, obtained from N = 68 selected patches (N = 8–13 per frequency) of an original N = 96 recorded patches, confirmed our initial qualitative observations and allowed us to quantify three specific features of transduction (Figure 2A).

Author Manuscript Author Manuscript Author Manuscript Author Manuscript

First, the amplitude of the initial peak current increased monotonically and steeply with stimulus frequency (Figure 2B): While a 0.5 Hz stimulus elicited only 9.6±1.6% of the current elicited by '*step1*' (N = 8), a 50 Hz stimulus elicited 70.6±3.3% (N = 9), revealing that Piezo1 is a poor transducer of the onset of low-frequency (< 2 Hz), but a particularly efficient transducer of the onset of high-frequency (> 20 Hz) sinusoidal stimuli.

Second, the amplitude of the last peak current showed a bimodal dependence on stimulus frequency (Figure 2B): Currents increased with frequency from 9.6±1.6% of '*step1*' at 0.5 Hz (N = 8) to a maximum of 23.5±4.0% at 10 Hz (N = 9) and then decreased to 10.1±1.1% at 50 Hz (N = 9). We also observed that the standard deviation of the last two seconds of individual current traces during sustained stimulation, which can be taken as a measure of how well individual current peaks from successive stimulation cycles can be distinguished, had a similar bimodal dependence on frequency with a maximum at ~10 Hz (Figure 2C). Thus, for sustained sinusoidal stimulations, Piezo1 functions as a bandpass filter with a center frequency of ~10 Hz.

Third, a 'tonic' current, remaining between successive peaks, developed monotonically with stimulus frequency (Figure 2B), increasing from nearly zero at 0.5 Hz to 3.4±0.4% at 50 Hz (N = 9). While the tonic current is small when compared to the current elicited by a single step pulse, it contributes to an integrated current that, while still being bimodal, has a shallower frequency dependence at high frequencies (> 10 Hz) than would be predicted from the last peak current amplitudes alone (Figure 2D). Together, these results demonstrate that Piezo1 functions both as a high-pass filter for detecting the onset of sinusoidal stimulations, as well as a bandpass filter that becomes particularly inefficient at faithfully transducing individual stimulation maxima during sustained high stimulation frequencies (> 20 Hz).

We next reasoned that the specific aspects of Piezo1 transduction we observed thus far arise due to the stimulus waveform. That is, in addition to the periodicity, the speed of onset and offset of a single cycle within the stimulus might affect transduction efficiency. We therefore measured Piezo1 currents elicited by repetitive square pulse stimuli. Specifically, during the four second test period, we periodically applied brief (30 ms) pressure steps (from +5 to −50 mmHg) at frequencies of 0.5, 1, 2, 5, and 10 Hz (Figure 3A). Importantly, the 30 ms stimulus allowed for full activation of Piezo1 currents, but little inactivation during the test pulse itself (Figure 3A, 10 Hz inset). Unlike for the sinusoidal stimulus, where the mean pressure over four seconds (−22.5 mmHg) was independent of stimulus frequency, for a square pulse stimulus, mean pressure increased with stimulus frequency (from +4.2 mmHg at 0.5 Hz to −28 mmHg at 20 Hz). Owing to this increased duration under pressure (as well as potentially the more abrupt transitions between pressures as compared to a sinusoidal waveform), we observed more current rundown at higher frequencies than with a sinusoidal stimulus and were therefore unable to collect high-quality data at frequencies greater than 10 Hz (Figure S1).

As before, we executed only one protocol per patch, then triaged and normalized the currents to compare N = 39 independent measurements (N = 7–11 per frequency; Figure 3A; Figure S1). Again, the currents elicited by this square pulse protocol varied dramatically

Author Manuscript Author Manuscript Author Manuscript Author Manuscript

with stimulus frequency and additionally, they were distinct from those elicited by sinusoidal stimulation.

First, the peak current amplitude evoked by the first pulse was similar at all frequencies (78.1±6.4% at 0.5 Hz (N = 8) and 93.4±10.5% at 10 Hz (N = 7); P=0.52, single-factor ANOVA) (Figure 3B). This result, while fully expected, shows that Piezo1 transduces the onset of a square pulse signal equally well across stimulation frequencies, which is drastically different from sinusoidal stimulation.

Second, the current amplitude of the last peak decreased monotonically with increasing stimulus frequency, from 63.8±7.8% at 0.5 Hz (N = 8) to 27.2±5.3% at 10 Hz (N = 7) (Figure 3B). This suggests that for a square pulse stimulus waveform, Piezo1 acts as a low-pass filter, failing to efficiently transduce continuous stimulation at higher frequencies. Interestingly, at 10 Hz, the peak current amplitude during the last cycle was not significantly different from that for a sinusoidal stimulus (sinusoidal: 23.5±4.0%, N = 9; square pulse: 27.2±5.3%, N = 7, P=0.58, Student's t-test), consistent with the idea that at high frequencies, stimulus durations and rise/fall times of single square pulses and single sinusoidal cycles converge to similar values. These data indicate that Piezo1 transduction is highly dependent on the stimulus waveform at low stimulation frequencies (< 2 Hz), but that it only poorly discriminates between these two waveforms at high stimulation frequencies (> 10 Hz).

In summary, Piezo1 ion channels transduce distinct salient features of periodic stimulation, such as stimulus onset, stimulus duration, individual stimulus cycles, and stimulus waveform, all of which can be important aspects of a complex mechanical interaction, in a highly frequency-dependent manner.

A four state mechanism of channel gating reproduces Piezo1 frequency filtering

Based on two observations, we reasoned that the effects of stimulus frequency and waveform on Piezo1-mediated currents could be solely explained by changes in Piezo1 open probability. Specifically, we found that *i*) current amplitude levels of sporadic single-channel gating events we identified in our 50 Hz sinusoidal stimulation experiments were identical to previously published values for Piezo1 (35.1±1.7 pS; N = 3) (Figure S3) (Bae et al., 2013b; Coste et al., 2012; Wu et al., 2016a), and that *ii*) both in the absence of repetitive stimulation and at low stimulation frequencies, the ratios of current amplitudes between the initial and final test pulses '*step1*' and '*step2*' did not depend on stimulus frequency (Figure S1M), arguing that the only two other factors that determine total current, unitary conductance g and channel number N, are constant throughout our experiments. We next hypothesized that changes in open probability during repetitive stimulation could be largely explained by intrinsic Piezo1 channel gating properties (i.e., the pressure-dependent activation, and the time courses of inactivation and deactivation), and not by adaptation or by structural properties of the membrane.

A three state mechanism of channel gating, including one closed (C), one open (O), and one inactivated (I) state, has been previously proposed for Piezo channel function and is the minimal mechanism that can explain the distinct activation, inactivation, and deactivation time courses observed upon stimulation with a classical single pressure step (Bae et al.,

Author Manuscript Author Manuscript Author Manuscript Author Manuscript

2013a; Gottlieb et al., 2012). To test experimentally if current decay indeed results from inactivation, rather than adaptation, we first applied a 125 ms conditioning pressure-step to −30 mmHg to partially activate Piezo1 channels and allow for substantial current decay, followed by additional pressure steps from −40 to −100 mmHg, and compared current amplitudes to those evoked by a standard step protocol (Figure S4A–C). Little additional current was elicited following the conditioning step, even at pressures approaching lytic tension (31.4±3.4% at −100 mmHg; N = 11). This result reveals a small contribution of adaptation to Piezo1 current decay, as was previously found for rapidly-adapting mechanosensitive currents in DRG neurons (Hao and Delmas, 2010), but also demonstrates that the predominant mechanism for current decay is inactivation.

Next, we probed for the presence of additional inactivated states with a two-step protocol with varied time-delay from 10 ms to 41 s. We found that the time-dependence of current recovery was well-fit with two exponentials of 24±7 ms and 10.2±2.0 s, consistent with two kinetically distinct states contributing to channel inactivation, and accordingly incorporated two inactivated states into our model (Figure S4D–F).

We also assumed pressure-dependent transitions from closed to open ($a(p) = a_0 \cdot \exp(-p/k)$) and from inactivated to closed states ($e(p) = e_0 \cdot \exp(p/k)$) while keeping other rate constants pressure-independent, which is in agreement with previous models and our own functional data (Bae et al., 2013a; Gottlieb et al., 2012) (Figure 4A): Specifically, with a protocol measuring current decay at pressures ranging from +5 to −40 mmHg following a brief step to −50 mmHg to open channels, we found that the time course of both deactivation (open to closed) and inactivation (open to inactivated) showed little pressure dependence as compared to activation (Figure S4G–I). We then developed a computer script in IgorPro (Wavemetrics) designed to simulate current responses to sinusoidal stimuli at different frequencies, and by comparison to the experimental data, converge towards optimal numerical solutions for the eight rate constants associated with a four state model (Methods).

By simultaneously fitting data at 2, 5, 10, and 20 Hz, where data quality and signal-to-noise ratio were highest, we found the data were best fit by a model incorporating a second inactivated state reached from the open state, and obtained rate constants of $a = 5.1\ s^{-1}$, $b = 116.9\ s^{-1}$, $c = 8.0\ s^{-1}$, $d = 0.4\ s^{-1}$, $e = 34.6\ s^{-1}$, $f = 33.6\ s^{-1}$, $g = 4.0\ s^{-1}$, $h = 0.6\ s^{-1}$, $k = 6.8$ mmHg. Simulations using these values recapitulated the experimentally recorded currents in response to sinusoidal stimuli, with an average residual across all frequencies (0.5 – 50 Hz) of 1.9% (Figure 4B). Notably, our simulations also identified a second solution with a similarly low average residual (2.0%), in which the second inactivated state is reached from the first inactivated state, highlighting that the precise sequence of allosteric transitions associated with inactivated states is still ambiguous.

Importantly, the optimal rate constants stated above accurately predict three key features of Piezo1 frequency filtering in the range of 0.5 – 50 Hz: the monotonic increase in first peak current and in tonic current with stimulation frequency, and the biphasic dependence of the last peak current amplitude on stimulation frequency (Figure 4D). We also evaluated the model by simulating all other stimulus protocols we tested experimentally, and found it captured every key feature of Piezo1 gating, including the response to a single saturating

Author Manuscript Author Manuscript Author Manuscript Author Manuscript

pressure step; the pressure-response (P_{50}) curve, the pressure-independence of deactivation and inactivation, and the time-course of recovery from inactivation (Figure S5A–H). The model also recapitulates the monotonic decrease in last peak amplitude with a square pulse protocol, as well as the phase shift with respect to the stimulus for a sinusoidal protocol (Figure S5I–K). Together, these results demonstrate that a four state mechanism of Piezo1 gating is sufficient to explain the transduction of periodic sinusoidal stimulations over four seconds and a frequency range of two orders of magnitude, as well as other key features of Piezo1 gating.

Encouraged by this validation, we next simulated Piezo1 responses to sinusoidal stimulations at frequencies that are not accessible experimentally (> 50 Hz) (Figure 4C–D). The results show that for high stimulation frequencies (up to 1 kHz) the first peak amplitude saturates at 94%, while both the last peak current and the tonic current reach a plateau of 13% and 12%, respectively. Thus, at very high frequencies, Piezo1 remains a good detector of the onset of periodic sinusoidal stimulations, whereas during a continuous stimulus, it conducts only a tonic current with little information about the stimulus phase.

We next reasoned that for Piezo channels to efficiently transduce phase information, the peak-to-peak amplitude of the current must be greater than its standard deviation (see Methods). We therefore took into account the stochastic nature of gating and examined the effect of channel number (N) on transduction. Assuming a membrane potential of V = −80 mV, we found that for N = 25 Piezo1 ion channels (g = 30 pS), variance dominates the peak-to-peak amplitude throughout nearly the entire frequency spectrum (0.5 – 1,000 Hz), whereas N = 100 channels are sufficient to discriminate phase information for intermediate frequencies (2 – 20 Hz) and N = 1,000 channels are sufficient to discriminate phase information throughout an even wider frequency spectrum (0.5 –100 Hz), failing only when the amplitudes of the tonic and phasic currents have nearly converged (Figure 4E). Together, these simulations and calculations show that for stimulation frequencies of 1 – 100 Hz, large ensembles of Piezo1 ion channels are indeed capable of transducing information about stimulus phase.

Inactivation is the mechanism of frequency filtering

We hypothesized that frequency filtering of Piezo1 was dictated, at least in part, by inactivation properties of the channel. To test this prediction, we took advantage of the fact that at positive potentials, Piezo1 inactivation is nearly eliminated (and deactivation is slowed) (Figure 5A) (Coste et al., 2010). We therefore measured the responses of Piezo1 upon sinusoidal stimulation at 0.5, 10, and 50 Hz at a holding potential of +80 mV (Figure 5B).

Depolarization had several effects on the frequency filtering of Piezo1: First, the amplitude of the first peak current varied only slightly with stimulus frequency (0.5 Hz: 80.5±2.3%, N = 6; 10 Hz: 92.5±2.6%, N = 6; 50 Hz: 91.0±2.5%, N = 6; P<0.01, single-factor ANOVA; Figure 5C). Second, at all frequencies, peak current amplitudes remained consistently high for the duration of the stimulus (last peak height: 0.5 Hz: 78.9±3.3%, N = 6; 10 Hz: 90.1±4.2%, N = 6; 50 Hz: 79.3±3.1%, N = 6; P=0.07, single-factor ANOVA). Third, the buildup of tonic currents at high stimulus frequencies was much higher than at negative

Author Manuscript Author Manuscript Author Manuscript Author Manuscript

potentials (10 Hz: 58.6±2.5%, N = 6; 50 Hz: 67.2±2.7%; N = 6). The large, stable peak currents at all frequencies are consistent with minimal accumulation of inactivation during repetitive stimulation at all frequencies, whereas the large tonic current likely results not only from minimal inactivation, but also from slowed deactivation, such that channels do not quickly return to closed states upon removal of the stimulus (Bae et al., 2013b). Together, these data demonstrate that, in the absence of inactivation, Piezo1 can reliably transduce mechanical stimuli at frequencies of up to at least 50 Hz equally well, and therefore inactivation is required for generating frequency filtering. They also confirm that at all frequencies, the sinusoidal pressure stimulus induces sufficient membrane tension to fully activate Piezo1, and therefore changes in frequency-dependent filtering arise from intrinsic channel properties, rather than from failure of the membrane to efficiently transduce the stimulus.

To further examine the link between inactivation and frequency filtering, we turned our attention to Piezo2, in which two channelopathies that differentially affect inactivation were previously identified in human patients, both of which cause distal arthrogryposis type 5 (Coste et al., 2013; McMillin et al., 2014). Specifically, mutation I802F accelerates recovery from inactivation, while mutation E2727del both slows the onset and accelerates the recovery from inactivation (Coste et al., 2013).

Because negative pressure is not an efficient activating stimulus for Piezo2, we changed our assay and used a blunt glass probe to indent the cell in a whole-cell recording (Coste et al., 2010; Coste et al., 2015). The stimulus was a periodically applied 10 ms square pulse (9.1±1.2 μm indentation) at frequencies of 1, 5, 20, and 40 Hz, which is the upper limit imposed by the speed of the piezoelectric driver. Again, the stimulus had a total duration of four seconds at all frequencies, and was framed by two standard 10 ms test pulses (‘$step_1$’ and ‘$step_2$’). Since we did not routinely observe rundown of currents in this configuration, we tested all frequencies once on each cell.

Wild-type Piezo2 responses to a square waveform stimulus were filtered such that the first peak amplitude was unaffected by stimulus frequency, but the amplitude of the last peak decreased steeply and monotonically with stimulus frequency, from 93.4±2.0% at 1 Hz to 7.1±2.4% at 40 Hz (N = 10) (Figure 6A–C). Thus, independent experiments (albeit using two different stimulation methods) demonstrate that both Piezo1 and Piezo2 can reliably detect the onset of repetitive square pulse stimulations at all frequencies, but that they function as low-pass filters for continuous stimulation.

Next, we individually introduced each mutation into mouse Piezo2 and compared their responses to wild-type channels. At low frequencies (1 Hz), responses of I802F and E2727del were indistinguishable from wild-type Piezo2 (wild-type: 93.4±2.0%, N = 10; I802F: 94.2±4.8%, N = 11, P=0.89 vs. wild-type; E2727del: 93.2±2.3%, N = 9, P=0.94 vs. wild-type; Student’s t-test). However, both mutants transduced sustained stimuli at high frequencies more efficiently: at 40 Hz, the amplitudes of the last peak current were substantially higher for I802F (16.6±6.1%; N = 11) and E2727del (19.1±2.5%; N = 9) as compared to wild-type Piezo2 (7.1± 2.4%; N = 10; P=0.18 vs. I802F and P<0.01 vs. E2727del; Student’s t-test) (Figure 6A, C). Thus, Piezo2 channels with these human disease-

Author Manuscript Author Manuscript Author Manuscript Author Manuscript

related point mutations, while still functioning as low-pass filters, have attenuated frequency filtering. Moreover, the fact that E2727del is a more efficient transducer of sustained stimulations at high frequencies than I802F is consistent with a mechanism by which both entry into and recovery from inactivation shape frequency filtering.

Frequency filtering of Piezo2 is conserved in rapidly-adapting DRG neurons

In DRG neurons, the rapidly-adapting (RA) mechanosensitive current is mediated by Piezo2 (Ranade et al., 2014b). To test whether frequency filtering was conserved in cells natively expressing Piezo2 channels, we first mechanically stimulated isolated and cultured RA DRG neurons using a blunt glass pipette with repetitive 10 ms square pulses (17.3±2.5 μm indentation) at 1, 5, 20, and 40 Hz and measured the currents evoked in voltage-clamp (Figure 7A). The time course of inactivation (τ) during an isolated single step pulse '$step_1$' was similar to the values from our own recordings with wild-type mouse Piezo2 in HEK293t cells (DRG: 3.1±0.3 ms, N = 7; HEK293t: 2.0±0.4 ms, N = 10; P=0.059, Student's t-test) and was well within the typical classification of RA currents for every cell (<10 ms) (Ranade et al., 2014b). More importantly, the currents evoked by repetitive stimulations were identical to those observed in HEK293t cells transiently expressing Piezo2 (Figure 6A). Specifically, at 40 Hz, current amplitudes of the last peak were indistinguishable (HEK293t: 7.1±2.4%, N = 10; DRG: 13.1±2.0%, N = 7, P=0.095, Student's t-test) (Figure 7B). Both measurements are consistent with the notion that neurons we recorded from are Piezo2-expressing and that Piezo2 frequency filtering is unaltered by differences in cellular environment between HEK293t cells and DRG neurons in this frequency range and over this stimulus duration.

For excitable cells to discriminate distinct mechanical stimulations, a receptor potential must be sufficient to initiate an action potential. We therefore tested how repetitive mechanical stimulations at different frequencies evoked action potential firing in DRG neurons. For each neuron, we first confirmed the presence of RA mechanosensitive currents in a voltage-clamp configuration (Figure 7C). Next, we chose stimulus intensities that reliably elicited action potentials at a stimulus frequency of 1 Hz. Finally, the same stimulus intensity was used to test firing behavior on the same cell at 5 Hz and 20 Hz (Figure 7D). We found that at higher frequencies, neurons did not retain the consistent firing observed at 1Hz. Instead, they fired action potentials only 4–5 times at 5 Hz and only 1–2 times at 20 Hz, before failing to fire in response to subsequent stimuli (Figure 7E). Interestingly, at 5 Hz, several neurons faithfully followed the mechanical stimulus for the first 4–5 stimuli and then showed intermittent firing later in the stimulus, suggesting the receptor potentials had fallen to near-threshold. We quantified these subthreshold depolarizations at 5 Hz and 20 Hz (excluding any stimulus that elicited an action potential) (Figure 7F). As predicted from the frequency filtering by Piezo2-mediated currents in both HEK293t cells and in DRG neurons in voltage-clamp, both 5 Hz and 20 Hz stimuli led to smaller depolarizations later in the stimulus, with a more rapid decline in depolarization for 20 Hz (amplitude of last depolarization for 5 Hz: 12.3±1.7 mV; 20 Hz: 4.3±1.0 mV; N = 4; P<0.05; paired t-test). Therefore, the ability of Piezo2 to act as a low-pass filter in response to repetitive stimulations is conserved in RA DRG neurons.

Author Manuscript Author Manuscript Author Manuscript Author Manuscript

Discussion

Mechanosensitive cells are exposed to repetitive mechanical stimulations that vary over a wide range of frequencies: For example, successive heart contractions cause arterial blood flow that elicits pulsatile shear stress on endothelial cells at 0.5 – 3 Hz (Hong et al., 2014; Spronk et al., 2005), whereas sinusoidal sound waves deflect hair cells of the inner ear at frequencies of up to 20,000 Hz (LeMasurier and Gillespie, 2005), and the sweeping motion of a fingertip during texture sensing causes repetitive mechanical stimulations of Merkel cells and DRG neurons in the skin whose frequency depends on both motion speed and surface texture (BensmaIa and Hollins, 2003; Scheibert et al., 2009). A crucial first step in transduction of these complex mechanical stimuli is the opening of a mechanosensitive ion channel (Haswell et al., 2011; Ranade et al., 2015). Here, we characterize and explain mechanistically how two mechanosensitive ion channels, Piezo1 and Piezo2, transduce complex repetitive mechanical inputs in a heterologous expression system.

Our data reveal that Piezo ion channels act as frequency filters of both the onset and continuation of repetitive mechanical stimuli. The effects are substantial in size, with Piezo1 transduction efficiencies ranging from 10% to 71% for onset of a sinusoidal stimulus, and 10% to 24% for continuous stimulation, acting over a frequency bandwidth of at least two orders of magnitude (0.5 – 50 Hz). Most importantly, our measurements reveal the transduction limits of Piezo ion channels, which turn out to be poor discriminators and inefficient transducers of continuous high-frequency stimulations. Moreover, our calculations directly predict that specific aspects of signal transfer depend on, in addition to intrinsic channel gating (P_o), the number of stimulated channels (N). Specifically, for Piezo1, phase information of a periodic sinusoidal stimulus can be faithfully transduced at intermediate frequencies (1 – 100 Hz) with an ensemble of ~100 channels, but is lost if fewer than ~25 channels participate in transduction (Figure 4). Of course, endogenous channel numbers range widely; while previous studies have reported activation of ~100 channels in single mechanosensitive Merkel cells and in rapidly-adapting DRG neurons *in situ*, the spatial organization of channels on distal processes and the intensity of the stimulus will all affect the number of channels that are synchronously activated (Hao and Delmas, 2010; Ikeda et al., 2014; Jia et al., 2013).

Several pieces of evidence in our study support that channel inactivation underlies frequency filtering: First, we demonstrate that a four state model of channel gating (closed, open, and two inactivated states) is sufficient to recapitulate not only basic kinetic gating properties, but also Piezo1 frequency filtering of a sinusoidal stimulus over two orders of magnitude, including an increased efficiency of detection of onset of stimulation at higher frequencies as well as a bimodal dependence of last peak amplitude with frequency (Figure 4). However, we cannot conclusively place the second inactivated state as originating from the open state, nor can we rule out the existence of additional kinetically distinct states, largely because our 4 s stimulation protocol does not adequately probe slower transitions. Indeed, the “rundown” of currents that we and other laboratories observe upon repeated mechanical stimulation is only partially explained by the longer time constant of recovery from inactivation we observed (10.2 s), potentially indicating the presence of yet another, extremely long-lived inactivated state (Figure S1) (Bae et al., 2013a; Wu et al., 2016a). Extending the duration of

Author Manuscript Author Manuscript Author Manuscript Author Manuscript

stimulus protocols substantially will be challenging however, since the reversibility of membrane geometry and thus tension is undermined by membrane creep inside the patch pipette, which has been shown to increase over time (Slavchov et al., 2014; Suchyna et al., 2009).

Second, we showed that destabilizing inactivation affected frequency filtering. When we removed inactivation from Piezo1 via depolarization, frequency filtering was eliminated entirely (Figure 5). Moreover, even a relatively minor change in inactivation kinetics (owing to mutations linked to distal arthrogryposis type 5) modulated frequency filtering in Piezo2 (Figure 6).

Inactivation thus serves as a key locus for modulation of frequency filtering. The fact that extracellular pH, divalent cation concentration, temperature, and bradykinin are all predicted to alter the time course of Piezo inactivation directly points at these factors as potential physiologically relevant regulators of frequency filtering (Bae et al., 2015; Dubin et al., 2012; Gottlieb et al., 2012). For example, under inflammatory conditions, a reduction in pH will stabilize inactivation, whereas elevated bradykinin levels will slow it. An intricate balance between competing mechanisms will thus influence the efficiency of Piezo2 in sensory DRG neurons in transducing continuous repetitive stimuli, which could be one component adding to increased mechanical sensitivity upon injury. Minor changes in inactivation kinetics will likely have the largest effect in cells with high input resistance, such as Merkel cells, where a relatively small steady-state current (<20% of the peak current) can induce sufficient depolarization to sustain firing (Ikeda et al., 2014). Intriguingly, inactivation kinetics are not apparently affected by stimulus intensity, perhaps providing a mechanism by which Piezo-expressing cells can maintain the same filtering properties regardless of stimulus intensity (Coste et al., 2010).

Of course, the ability of ion channels to convey frequency filtering is not unique to Piezos: Neurotransmitter receptors nAChR, GlyR and AMPAR desensitize quickly upon ligand binding and exhibit a pronounced frequency-dependent responsiveness (Papke et al., 2011), whereas ASIC channels, which desensitize slowly, transduce high frequency stimulations more efficiently (MacLean and Jayaraman, 2016). Our study extends this concept to mechanotransduction, where the notion of repetitive stimulation (e.g. by sound, vibrations, or texture sensing) is arguably of high relevance. In fact, the role of desensitization as an essential mechanism in shaping firing of mechanosensory neurons, and achieving specialization in responses to diverse touch stimuli, has previously been well-appreciated (Hao and Delmas, 2010; Rugiero et al., 2010). Our data provide further evidence that Piezo2 contributes to this specialization, as we were able to measure action potential firing in RA DRG neurons that was consistent with the frequency-dependent current profile of Piezo2 (Figure 7).

Although the stimulus waveforms we tested (sinusoidal and step-like) are idealized, they are likely good representations of physiologically relevant mechanical inputs. For example, acoustic sound and vibrations are sinusoidal by nature, as is the slipping of the ridges of our fingerprints over microscopic obstacles on a textured surface (BensmaIa and Hollins, 2003) (Figure 1A), whereas the sharp waveform of pulsatile flow in arteries is well-approximated

Author Manuscript Author Manuscript Author Manuscript Author Manuscript

by a step-like waveform (Hong et al., 2014). We can further speculate that intrinsic filtering by Piezo ion channels contributes to several physiological mechanotransduction processes, while it might be less relevant to others: For example, in a two-plate choice assay, mice appear insensitive to ongoing vibrations of 150 Hz, but show a marked aversion to pulsating vibration (with a cycle of three seconds on, two seconds off) – a phenotype that is entirely dependent on Piezo2 (Ranade et al., 2014b). Moreover, Merkel cells, in which the rapidly-adapting mechanosensitive current is mediated by Piezo2, are sensitive only to vibrations at very low frequencies (<10 Hz) (Ikeda et al., 2014; Woo et al., 2014). Both results are consistent with our data showing that fast (>20 Hz) repetitive stimuli are transduced well at their onset, but only inefficiently during continuous exposure, whereas slow repetitive stimuli (<2 Hz) are transduced faithfully over seconds. In contrast, expression of Piezo1 in heart and arterial endothelial cells, along which mechanical forces from blood pressure oscillate sharply at frequencies of ~1 to ~3 Hz (60–180 heart beats per minute), will lead to consistent efficiency of transduction in this frequency range (Hong et al., 2014; Ranade et al., 2014a; Spronk et al., 2005). In the cardiovascular system, frequency-independent transduction may be advantageous to ensure a robust detection of pulses in blood pressure and flow with every heartbeat. In contrast, auditory transduction of tones from 8 to 20 kHz depends only little on Piezo2, which carries the reverse-polarity currents observed at the apical surface of outer hair cells during development (Wu et al., 2016c). This is consistent with our finding that Piezo2 is not particularly efficient at continuously transducing and discriminating high-frequency stimuli; at best, it could contribute to hearing by detecting the onset of auditory stimuli (Figure 6). Rather, our results suggest that other mechanotransducers with distinct kinetic properties, including either the lack of inactivation or the presence of ultra-rapid recovery from inactivation, are best-suited to transduce high-frequency stimuli.

Experimental Procedures

Piezo constructs

Mouse Piezo1-pIRES-EGFP in pcDNA3.1 was obtained from Ardem Patapoutian and previously described (Coste et al., 2012; Lewis and Grandl, 2015). Mouse Piezo2 was synthesized to be codon-optimized for expression in human cells by Genewiz (South Plainfield, NJ) and ligated into pcDNA3.1(+) between restriction sites Kpn1 and Not1. Mutation I802F and deletion E2727del were introduced using the Quikchange II XL site-directed mutagenesis kit (Agilent technologies, Santa Clara, CA) and constructs were fully sequence-verified.

Cell culture

Human embryonic kidney HEK293t cells (ACC CRL-11268; verified mycoplasma-free 10/19/2015) were grown in DMEM (Life technologies, Carlsbad, CA) with 10% heat-inactivated fetal bovine serum (Sigma-Aldrich), 50 units/ml penicillin, and 50 mg/ml streptomycin (Life Technologies). Cells were transfected 24–48 hours before recording with mouse Piezo1-pIRES-EGFP or co-transfected with wild-type or mutant mouse Piezo2 or pcDNA3.1(+) (empty vector) and GFP as previously described and detailed in Supplementary Experimental Procedures. DRG cultures were prepared as previously

Author Manuscript Author Manuscript Author Manuscript Author Manuscript

described (Xu et al., 2015). Briefly, DRG were removed from 4–7 week-old mice of either sex and tissues were digested with collagenase (1.25 mg/ml, Roche) and dispase-II (2.4 units/ml, Roche) for 90 min, followed by 0.25% trypsin for 8 minutes at 37°C. Cells were plated on glass cover slips coated with poly-D-lysine and laminin and grown in a neurobasal defined medium (with 2% B27 supplement) in the presence of 5 μM AraC for 24–72 hours before experiments.

Electrophysiology

Patch-clamp recordings were performed at room temperature as previously described (Coste et al., 2010; Lewis and Grandl, 2015) and detailed in Supplemental Experimental Procedures.

Mechanical stimulation

Mechanical stimulation was performed as previously described by using a high-speed pressure clamp system (HSPC-1; ALA Scientific Instruments, Farmingdale, NY) to apply negative pressure through the patch pipette or by indenting the cell with a fire-polished glass pipette controlled by a piezo-electric driver (E625 LVPZT Controller/Amplifier; Physik Instrumente) (Coste et al., 2010; Hao et al., 2013b; Lewis and Grandl, 2015). Details of the mechanical stimuli are available in Supplemental Experimental Procedures.

Data analysis

Analysis was performed with Igor Pro 6.22A (WaveMetrics, Lake Oswego, OR). Electrophysiological recordings were only analyzed for patches with a seal resistance of at least 1 GΩ and peak currents of at least 50 pA for cell-attached and 100 pA for whole-cell experiments. Baseline currents before mechanical stimulation were subtracted off-line. Cell-attached patches were triaged as described in Figure S1. For whole-cell experiments, cells in which '$step_2$' was <50% of '$step_1$' at any frequency were excluded (3 of 30 cells). In cell-attached recordings, peak and tonic currents elicited by frequency stimulation protocols were taken as the mean of 5 points including and surrounding the minimum/maximum current to reduce noise. Phase shift and FFT analysis were performed using the auto correlate function and complex FFT function, respectively, in IgorPro.

Gating model of Piezo1

The model of Piezo1 gating was built and fit using Igor Pro 6.22A; the custom code is available in our Github repository (github.com/GrandlLab) and details are available in Supplemental Experimental Procedures.

Statistical analysis

Statistical analyses were performed with paired or unpaired Student's t-test or one-way analysis of variance (ANOVA). All data are reported as mean±s.e.m. Significant thresholds were set as $P<0.05$, as described in the text.

Supplementary Material

Refer to Web version on PubMed Central for supplementary material.

Author Manuscript Author Manuscript Author Manuscript Author Manuscript

Acknowledgments

This study was supported by NIH F32NS094088 (AHL) and Duke University. We thank Yong-Ho Kim and Ru-Rong Ji at Duke University for providing DRG cultures and all members of the Grandl lab for thoughtful comments on the study.

References

Albuisson J, Murthy SE, Bandell M, Coste B, Louis-dit-Picard H, Mathur J, Feneant-Thibault M, Tertian G, de Jaureguiberry JP, Syfuss PY, et al. Dehydrated hereditary stomatocytosis linked to gain-of-function mutations in mechanically activated PIEZO1 ion channels (vol 4, pg 1884, 2013). Nature Communications 4. 2013

Bae C, Gnanasambandam R, Nicolai C, Sachs F, Gottlieb PA. Xerocytosis is caused by mutations that alter the kinetics of the mechanosensitive channel PIEZO1. Proc Natl Acad Sci U S A. 2013a; 110:E1162–1168. [PubMed: 23487776]

Bae C, Gottlieb PA, Sachs F. Human PIEZO1: removing inactivation. Biophys J. 2013b; 105:880–886. [PubMed: 23972840]

Bae C, Sachs F, Gottlieb PA. Protonation of the human PIEZO1 ion channel stabilizes inactivation. J Biol Chem. 2015; 290:5167–5173. [PubMed: 25561736]

BensmaIa SJ, Hollins M. The vibrations of texture. Somatosens Mot Res. 2003; 20:33–43. [PubMed: 12745443]

Chesler AT, Szczot M, Bharucha-Goebel D, Ceko M, Donkervoort S, Laubacher C, Hayes LH, Alter K, Zampieri C, Stanley C, et al. The Role of PIEZO2 in Human Mechanosensation. N Engl J Med. 2016; 375:1355–1364. [PubMed: 27653382]

Coste B, Crest M, Delmas P. Pharmacological dissection and distribution of NaN/Nav1.9, T-type Ca2+ currents, and mechanically activated cation currents in different populations of DRG neurons. J Gen Physiol. 2007; 129:57–77. [PubMed: 17190903]

Coste B, Houge G, Murray MF, Stitziel N, Bandell M, Giovanni MA, Philippakis A, Hoischen A, Riemer G, Steen U, et al. Gain-of-function mutations in the mechanically activated ion channel PIEZO2 cause a subtype of Distal Arthrogryposis. Proc Natl Acad Sci U S A. 2013; 110:4667–4672. [PubMed: 23487782]

Coste B, Mathur J, Schmidt M, Earley TJ, Ranade S, Petrus MJ, Dubin AE, Patapoutian A. Piezo1 and Piezo2 are essential components of distinct mechanically activated cation channels. Science. 2010; 330:55–60. [PubMed: 20813920]

Coste B, Murthy SE, Mathur J, Schmidt M, Mechioukhi Y, Delmas P, Patapoutian A. Piezo1 ion channel pore properties are dictated by C-terminal region. Nature Communications. 2015; 6:7223.

Coste B, Xiao B, Santos JS, Syeda R, Grandl J, Spencer KS, Kim SE, Schmidt M, Mathur J, Dubin AE, et al. Piezo proteins are pore-forming subunits of mechanically activated channels. Nature. 2012; 483:176–181. [PubMed: 22343900]

Dubin AE, Murthy S, Lewis AH, Brosse L, Cahalan SM, Grandl J, Coste B, Patapoutian A. Endogenous Piezo1 Can Confound Mechanically Activated Channel Identification and Characterization. Neuron. 2017; 94:266–270. e263. [PubMed: 28426961]

Dubin AE, Schmidt M, Mathur J, Petrus MJ, Xiao B, Coste B, Patapoutian A. Inflammatory signals enhance piezo2-mediated mechanosensitive currents. Cell Rep. 2012; 2:511–517. [PubMed: 22921401]

Eastwood AL, Sanzeni A, Petzold BC, Park SJ, Vergassola M, Pruitt BL, Goodman MB. Tissue mechanics govern the rapidly adapting and symmetrical response to touch. Proc Natl Acad Sci U S A. 2015; 112:E6955–6963. [PubMed: 26627717]

Gottlieb PA, Bae C, Sachs F. Gating the mechanical channel Piezo1: a comparison between whole-cell and patch recording. Channels (Austin). 2012; 6:282–289. [PubMed: 22790451]

Hao J, Delmas P. Multiple desensitization mechanisms of mechanotransducer channels shape firing of mechanosensory neurons. J Neurosci. 2010; 30:13384–13395. [PubMed: 20926665]

Author Manuscript Author Manuscript Author Manuscript Author Manuscript

Hao J, Padilla F, Dandonneau M, Lavebratt C, Lesage F, Noel J, Delmas P. Kv1.1 channels act as mechanical brake in the senses of touch and pain. Neuron. 2013a; 77:899–914. [PubMed: 23473320]

Hao J, Ruel J, Coste B, Roudaut Y, Crest M, Delmas P. Piezo-electrically driven mechanical stimulation of sensory neurons. Methods Mol Biol. 2013b; 998:159–170. [PubMed: 23529428]

Haswell ES, Phillips R, Rees DC. Mechanosensitive channels: what can they do and how do they do it? Structure. 2011; 19:1356–1369. [PubMed: 22000509]

Heidenreich M, Lechner SG, Vardanyan V, Wetzel C, Cremers CW, De Leenheer EM, Aranguez G, Moreno-Pelayo MA, Jentsch TJ, Lewin GR. KCNQ4 K(+) channels tune mechanoreceptors for normal touch sensation in mouse and man. Nat Neurosci. 2011; 15:138–145. [PubMed: 22101641]

Hong S, Jung Y, Yen R, Chan HF, Leong KW, Truskey GA, Zhao X. Magnetoactive sponges for dynamic control of microfluidic flow patterns in microphysiological systems. Lab Chip. 2014; 14:514–521. [PubMed: 24310854]

Hung WC, Yang JR, Yankaskas CL, Wong BS, Wu PH, Pardo-Pastor C, Serra SA, Chiang MJ, Gu Z, Wirtz D, et al. Confinement Sensing and Signal Optimization via Piezo1/PKA and Myosin II Pathways. Cell Rep. 2016; 15:1430–1441. [PubMed: 27160899]

Ikeda R, Cha M, Ling J, Jia Z, Coyle D, Gu JG. Merkel cells transduce and encode tactile stimuli to drive Abeta-afferent impulses. Cell. 2014; 157:664–675. [PubMed: 24746027]

Jia Z, Ikeda R, Ling J, Gu JG. GTP-dependent run-up of Piezo2-type mechanically activated currents in rat dorsal root ganglion neurons. Mol Brain. 2013; 6:57. [PubMed: 24344923]

LeMasurier M, Gillespie PG. Hair-cell mechanotransduction and cochlear amplification. Neuron. 2005; 48:403–415. [PubMed: 16269359]

Lewis AH, Grandl J. Mechanical sensitivity of Piezo1 ion channels can be tuned by cellular membrane tension. Elife. 2015; 4

Loewenstein WR, Skalak R. Mechanical transmission in a Pacinian corpuscle. An analysis and a theory. J Physiol. 1966; 182:346–378. [PubMed: 5942033]

Lukacs V, Mathur J, Mao R, Bayrak-Toydemir P, Procter M, Cahalan SM, Kim HJ, Bandell M, Longo N, Day RW, et al. Impaired PIEZO1 function in patients with a novel autosomal recessive congenital lymphatic dysplasia. Nature Communications. 2015; 6:8329.

MacLean DM, Jayaraman V. Acid-sensing ion channels are tuned to follow high-frequency stimuli. J Physiol. 2016; 594:2629–2645. [PubMed: 26931316]

McMillin MJ, Beck AE, Chong JX, Shively KM, Buckingham KJ, Gildersleeve HI, Aracena MI, Aylsworth AS, Bitoun P, Carey JC, et al. Mutations in PIEZO2 cause Gordon syndrome, Marden-Walker syndrome, and distal arthrogryposis type 5. Am J Hum Genet. 2014; 94:734–744. [PubMed: 24726473]

Morley SJ, Qi Y, Iovino L, Andolfi L, Guo D, Kalebic N, Castaldi L, Tischer C, Portulano C, Bolasco G, et al. Acetylated tubulin is essential for touch sensation in mice. Elife. 2016; 5

Nakayama Y, Slavchov RI, Bavi N, Martinac B. Energy of Liposome Patch Adhesion to the Pipet Glass Determined by Confocal Fluorescence Microscopy. J Phys Chem Lett. 2016; 7:4530–4534. [PubMed: 27791368]

Nonomura K, Woo SH, Chang RB, Gillich A, Qiu Z, Francisco AG, Ranade SS, Liberles SD, Patapoutian A. Piezo2 senses airway stretch and mediates lung inflation-induced apnoea. Nature. 2017; 541:176–181. [PubMed: 28002412]

Papke D, Gonzalez-Gutierrez G, Grosman C. Desensitization of neurotransmitter-gated ion channels during high-frequency stimulation: a comparative study of Cys-loop, AMPA and purinergic receptors. J Physiol. 2011; 589:1571–1585. [PubMed: 21300749]

Pathak MM, Nourse JL, Tran T, Hwe J, Arulmoli J, Le DT, Bernardis E, Flanagan LA, Tombola F. Stretch-activated ion channel Piezo1 directs lineage choice in human neural stem cells. Proc Natl Acad Sci U S A. 2014; 111:16148–16153. [PubMed: 25349416]

Qi Y, Andolfi L, Frattini F, Mayer F, Lazzarino M, Hu J. Membrane stiffening by STOML3 facilitates mechanosensation in sensory neurons. Nature Communications. 2015; 6:8512.

Ranade SS, Qiu Z, Woo SH, Hur SS, Murthy SE, Cahalan SM, Xu J, Mathur J, Bandell M, Coste B, et al. Piezo1, a mechanically activated ion channel, is required for vascular development in mice. Proc Natl Acad Sci U S A. 2014a; 111:10347–10352. [PubMed: 24958852]

Author Manuscript Author Manuscript Author Manuscript Author Manuscript

Ranade SS, Syeda R, Patapoutian A. Mechanically Activated Ion Channels. Neuron. 2015; 87:1162–1179. [PubMed: 26402601]

Ranade SS, Woo SH, Dubin AE, Moshourab RA, Wetzel C, Petrus M, Mathur J, Begay V, Coste B, Mainquist J, et al. Piezo2 is the major transducer of mechanical forces for touch sensation in mice. Nature. 2014b; 516:121–125. [PubMed: 25471886]

Robles L, Ruggero MA. Mechanics of the mammalian cochlea. Physiol Rev. 2001; 81:1305–1352. [PubMed: 11427697]

Rugiero F, Drew LJ, Wood JN. Kinetic properties of mechanically activated currents in spinal sensory neurons. J Physiol. 2010; 588:301–314. [PubMed: 19948656]

Scheibert J, Leurent S, Prevost A, Debregeas G. The role of fingerprints in the coding of tactile information probed with a biomimetic sensor. Science. 2009; 323:1503–1506. [PubMed: 19179493]

Slavchov RI, Nomura T, Martinac B, Sokabe M, Sachs F. Gigaseal mechanics: creep of the gigaseal under the action of pressure, adhesion, and voltage. J Phys Chem B. 2014; 118:12660–12672. [PubMed: 25295693]

Spronk S, den Hoed PT, de Jonge LC, van Dijk LC, Pattynama PM. Value of the duplex waveform at the common femoral artery for diagnosing obstructive aortoiliac disease. J Vasc Surg. 2005; 42:236–242. discussion 242. [PubMed: 16102620]

Suchyna TM, Markin VS, Sachs F. Biophysics and structure of the patch and the gigaseal. Biophys J. 2009; 97:738–747. [PubMed: 19651032]

Wang S, Chennupati R, Kaur H, Iring A, Wettschureck N, Offermanns S. Endothelial cation channel PIEZO1 controls blood pressure by mediating flow-induced ATP release. J Clin Invest. 2016; 126:4527–4536. [PubMed: 27797339]

Woo SH, Lukacs V, de Nooij JC, Zaytseva D, Criddle CR, Francisco A, Jessell TM, Wilkinson KA, Patapoutian A. Piezo2 is the principal mechanotransduction channel for proprioception. Nat Neurosci. 2015; 18:1756–1762. [PubMed: 26551544]

Woo SH, Ranade S, Weyer AD, Dubin AE, Baba Y, Qiu Z, Petrus M, Miyamoto T, Reddy K, Lumpkin EA, et al. Piezo2 is required for Merkel-cell mechanotransduction. Nature. 2014; 509:622–626. [PubMed: 24717433]

Wu J, Goyal R, Grandl J. Localized force application reveals mechanically sensitive domains of Piezo1. Nature Communications. 2016a; 7:12939.

Wu J, Lewis AH, Grandl J. Touch, Tension, and Transduction - The Function and Regulation of Piezo Ion Channels. Trends Biochem Sci. 2016b

Wu Z, Grillet N, Zhao B, Cunningham C, Harkins-Perry S, Coste B, Ranade S, Zebarjadi N, Beurg M, Fettiplace R, et al. Mechanosensory hair cells express two molecularly distinct mechanotransduction channels. Nat Neurosci. 2016c

Xu ZZ, Kim YH, Bang S, Zhang Y, Berta T, Wang F, Oh SB, Ji RR. Inhibition of mechanical allodynia in neuropathic pain by TLR5-mediated A-fiber blockade. Nat Med. 2015; 21:1326–1331. [PubMed: 26479925]

Zarychanski R, Schulz VP, Houston BL, Maksimova Y, Houston DS, Smith B, Rinehart J, Gallagher PG. Mutations in the mechanotransduction protein PIEZO1 are associated with hereditary xerocytosis. Blood. 2012; 120:1908–1915. [PubMed: 22529292]

Zimmerman A, Bai L, Ginty DD. The gentle touch receptors of mammalian skin. Science. 2014; 346:950–954. [PubMed: 25414303]

Author Manuscript Author Manuscript Author Manuscript Author Manuscript

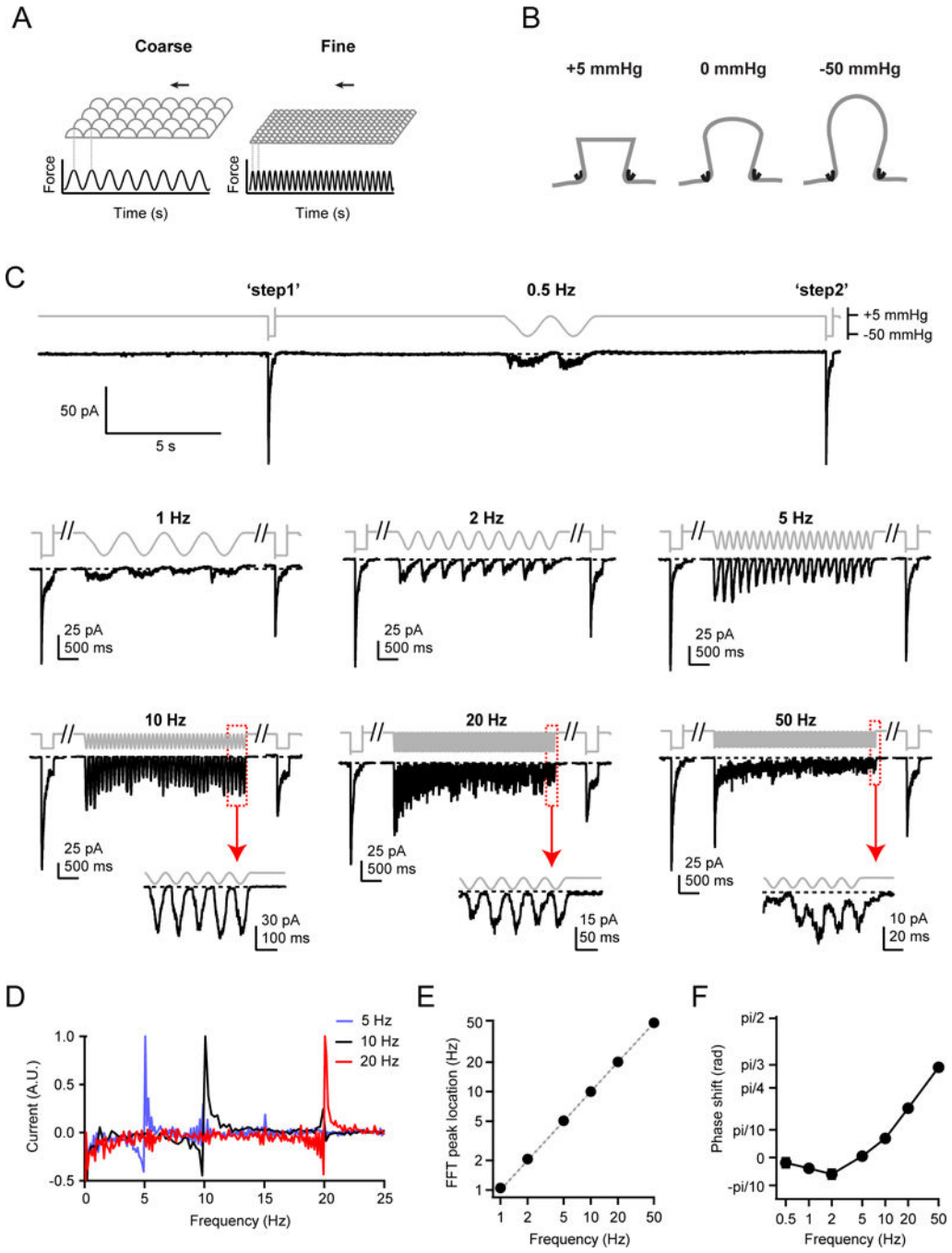

Figure 1. Repetitive sinusoidal pressure stimulation induces phase-locked oscillating inward currents in Piezo1-expressing HEK293t cells

(A) Schematic depicting two possible stimulus patterns (force over time) sensed by a fingertip brushing over a textured surface. (B) Schematic showing cell-attached high-speed pressure-clamp experiments, in which a small positive pressure (+5 mmHg) minimizes membrane curvature and Piezo1 open probability, while a large negative pressure (−50 mmHg) induces small curvature and high membrane tension and maximal Piezo1 open probability (Lewis and Grandl, 2015). (C) Stimulus protocols and representative raw currents from cell-attached patches from HEK293t cells transiently transfected with Piezo1.

Author Manuscript Author Manuscript Author Manuscript Author Manuscript

4 s sinusoidal pressure cycles oscillating between +5 and −50 mmHg at frequencies from 0.5 Hz to 50 Hz were applied. Dashed lines are zero current levels. Insets show magnifications of the last five pressure cycles at 10, 20 and 50 Hz. Each current trace is from a separate cell-attached patch. (D) Fast-Fourier transformations (FFT) of the 5 Hz, 10 Hz, and 20 Hz current traces from (C). (E) Average FFT maxima locations as a function of stimulus frequency (N = 68 cells). Error bars are obscured by data points. Dashed grey line represents unity, not a fit to the data. (F) Phase shift of currents relative to pressure stimulus for the last 2 s of stimulation. Error bars are obscured by data points. *See also* Figures S1, S2, S3.

Author Manuscript Author Manuscript Author Manuscript Author Manuscript

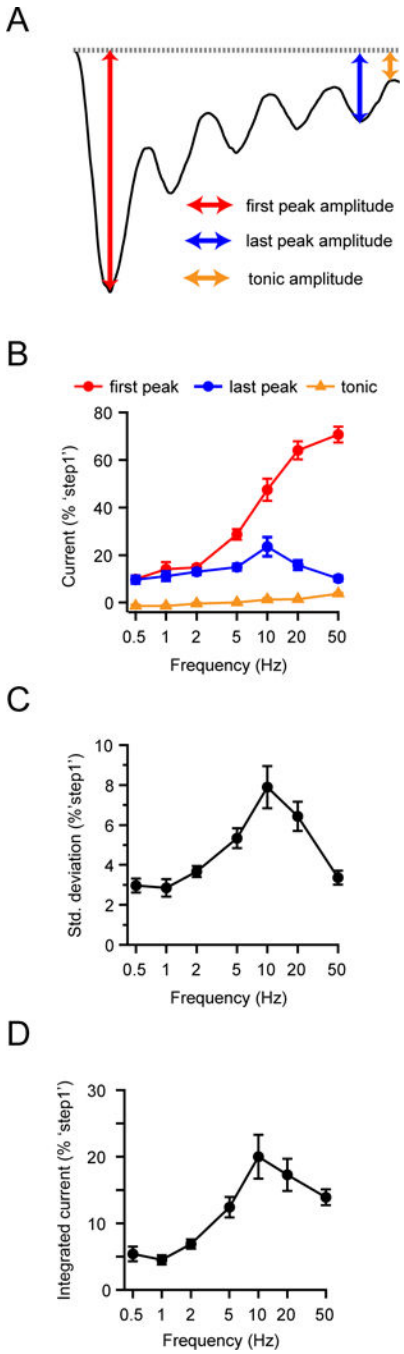

Figure 2. Piezo1 channels function as bandpass filters of sinusoidal pressure stimuli

(A) Illustration of current trace with time points for '*first peak*' (red), '*last peak*' (blue) and '*tonic current*' (orange) highlighted. (B) Mean amplitudes of the '*first peak*', '*last peak*', and '*tonic current*' of HEK293t cells transiently transfected with Piezo1 as a function of sinusoidal pressure stimulus frequency. All currents were individually normalized to the peak current of '*step1*' (see Figure 1C). (C) Standard deviation of current during the last two s as a function of stimulus frequency, normalized to peak amplitude of '*step1*'. All data are mean ± s.e.m.; N = 8–13 cells per frequency. (D) Integrated current during the last two s of a

four s sinusoidal pressure stimulus, as a function of frequency, normalized to the peak current of '*step1*'. *See also* Figure S1.

Author Manuscript Author Manuscript Author Manuscript Author Manuscript

Author Manuscript Author Manuscript Author Manuscript Author Manuscript

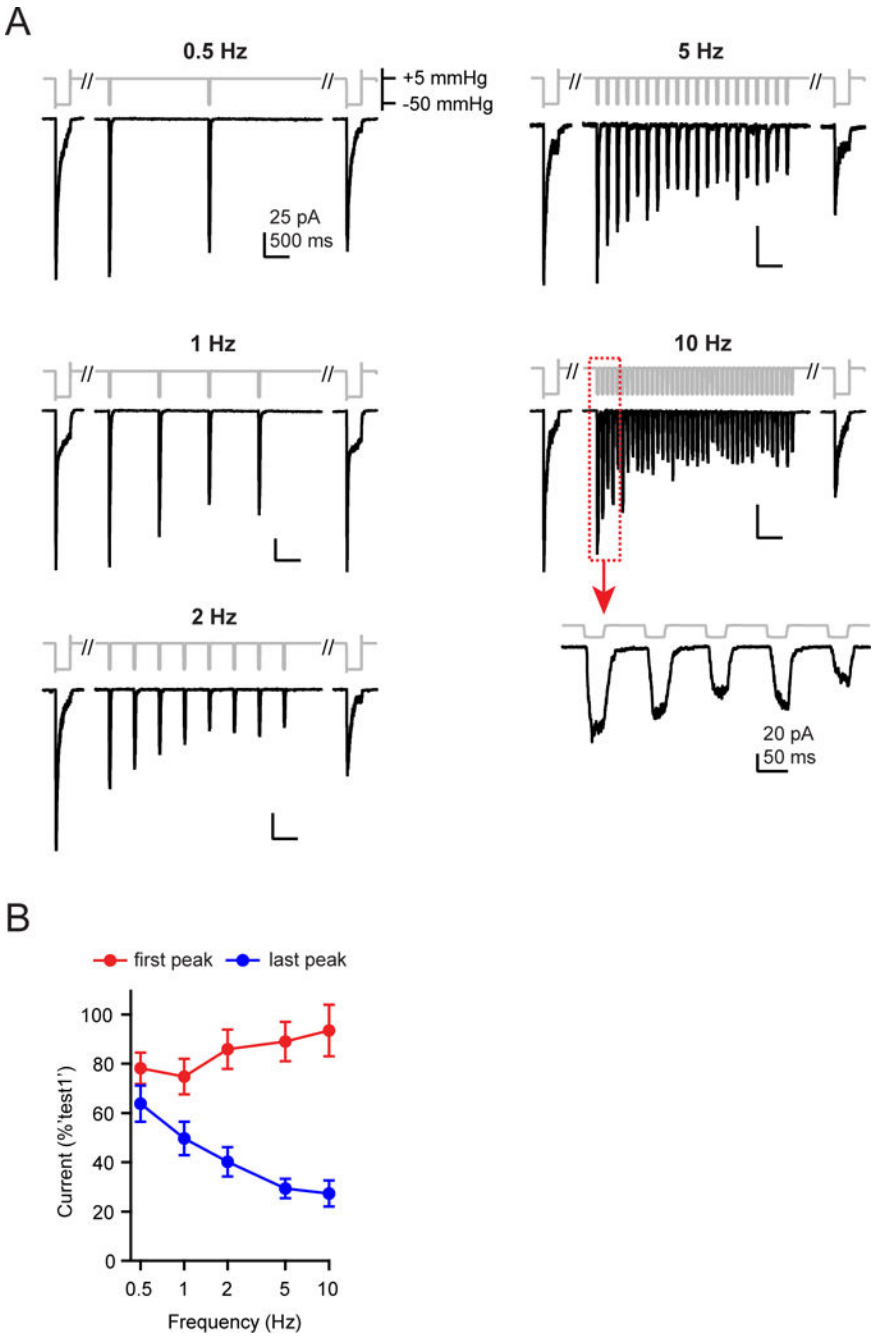

Figure 3. Piezo1 channels function as low-pass filters of square pulse pressure stimuli

(A) Repetitive square pulse pressure protocols (30 ms at −50 mmHg, varying times at +5 mmHg) and representative raw currents from HEK293t cells transiently transfected with Piezo1. Scale bars (25 pA, 500 ms) apply to all traces except 10 Hz inset (20 pA, 50 ms). (B) Mean amplitudes of the '*first peak*' (red circles) and '*last peak*' (blue circles) currents, normalized to the peak amplitude of '*step1*'. All data are mean ± s.e.m. N = 7–11 cells per frequency. *See also* Figures S1, S5.

Author Manuscript Author Manuscript Author Manuscript Author Manuscript

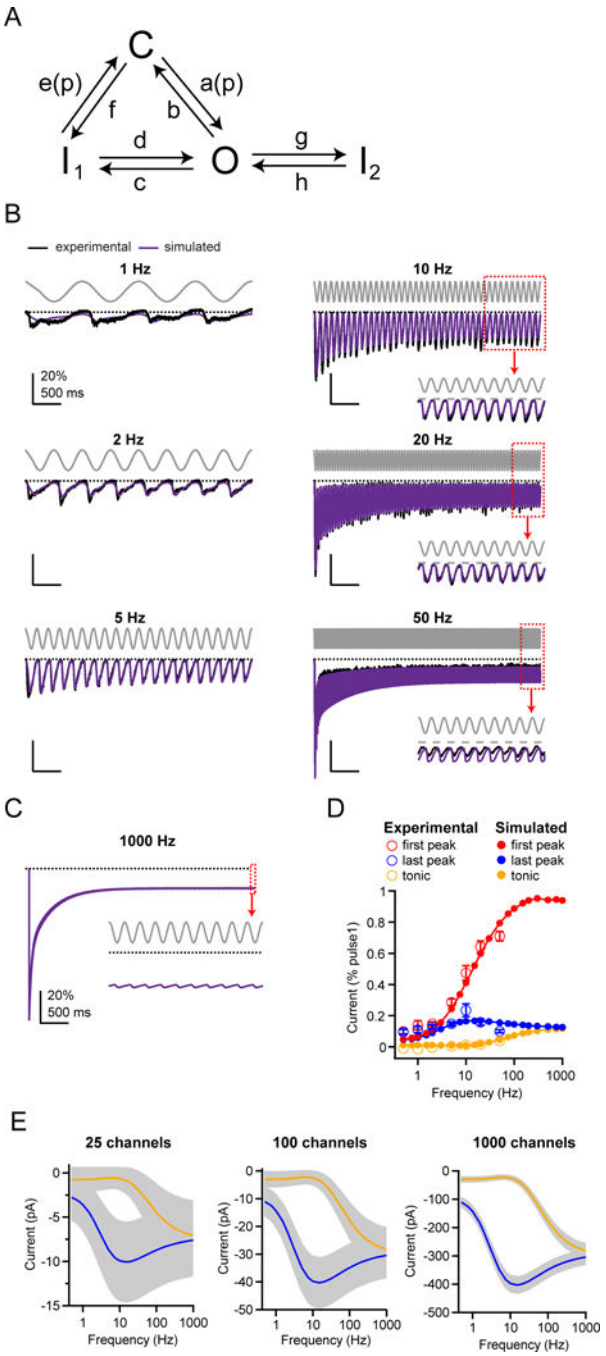

Figure 4. A three state gating mechanism describes Piezo1 frequency filtering

(A) Schematic for a four state gating mechanism for Piezo1, with arrows indicating transitions between open (O), closed (C) and two inactivated states (I_1 and I_2). Rate constants $a(p) = a_0 \cdot \exp(-p/k)$ (closed to open) and $e(p) = e_0 \cdot \exp(p/k)$ (inactivated to closed) are pressure-dependent. (B) Stimulus protocol (gray), normalized and averaged experimental currents from HEK293t cells transiently transfected with Piezo1 elicited by a sinusoidal pressure stimulus (see Figure 1) (black) and corresponding simulated currents using the best fit to the model in (A) (purple). Dashed line represents zero current. Insets show

Author Manuscript Author Manuscript Author Manuscript Author Manuscript

magnifications of the last pressure cycles. (C) Simulated current response for a 1 kHz sinusoidal pressure stimulus. Inset shows magnifications of the last pressure cycles. (D) Experimental and simulated mean amplitudes of the '*first peak*' and '*last peak*' currents and '*tonic*' current, normalized to '*step1*', as a function of stimulus frequency. (E) Simulated current amplitudes for mean "*last peak*" (solid black lines) and "*tonic*" currents (dashed black lines) and coefficient of variation (gray shading) as a function of stimulus frequency for N = 25, 100, and 1000 channels. Coefficient of variation was calculated as $\frac{\sigma}{\langle I \rangle} = \sqrt{\frac{1-q}{Nq}}$, where q is open probability and I = N*g*V is current. Currents were calculated with a single-channel conductance of 30 pS and a holding potential of −80mV (Coste et al., 2012). *See also* Figures S4, S5.

Author Manuscript Author Manuscript Author Manuscript Author Manuscript

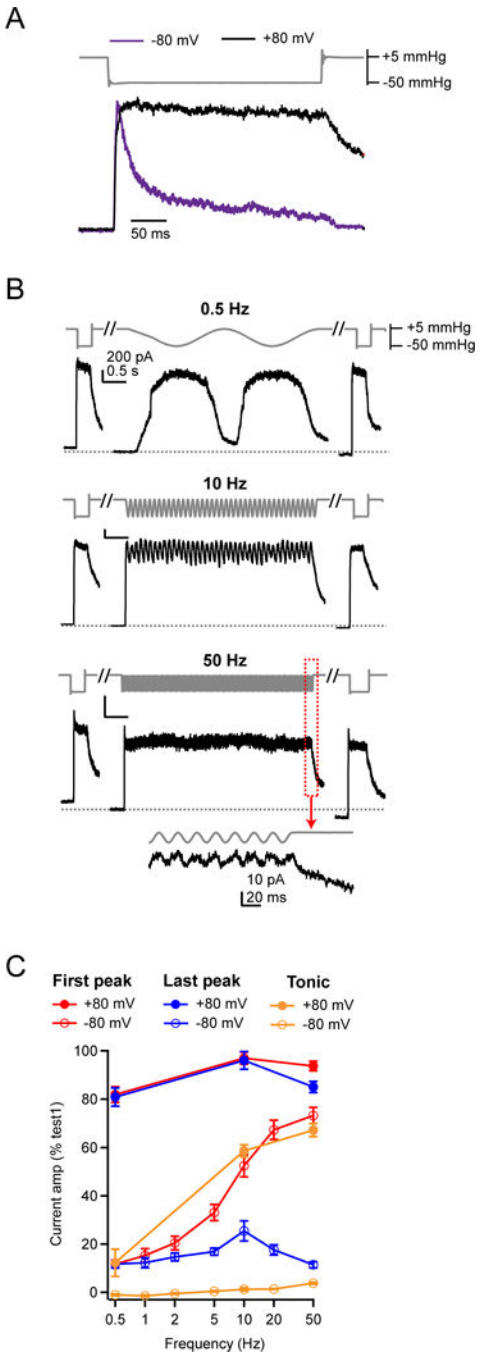

Figure 5. Inactivation is required for Piezo1 frequency filtering

(A) Stimulus protocol (gray) and representative currents in response to a static, 300 ms negative pressure step from two HEK293t cells transiently transfected with Piezo1 in cell-attached patches held at −80 mV (purple, inverted for ease of comparison) and +80 mV (black). Currents are normalized to their peak. (B) Sinusoidal stimulus protocol and representative outward currents from cell-attached patches held at +80 mV. Scale bar (200 pA, 0.5 s) applies to all three traces. (C) Mean amplitudes of the '*first peak*' and '*last peak*'

current as a function of stimulus frequency. Currents are normalized to the peak amplitude of '*step1*'. All data are mean ± s.e.m.; N = 6–13 cells per stimulus frequency.

Author Manuscript Author Manuscript Author Manuscript Author Manuscript

Author Manuscript Author Manuscript Author Manuscript Author Manuscript

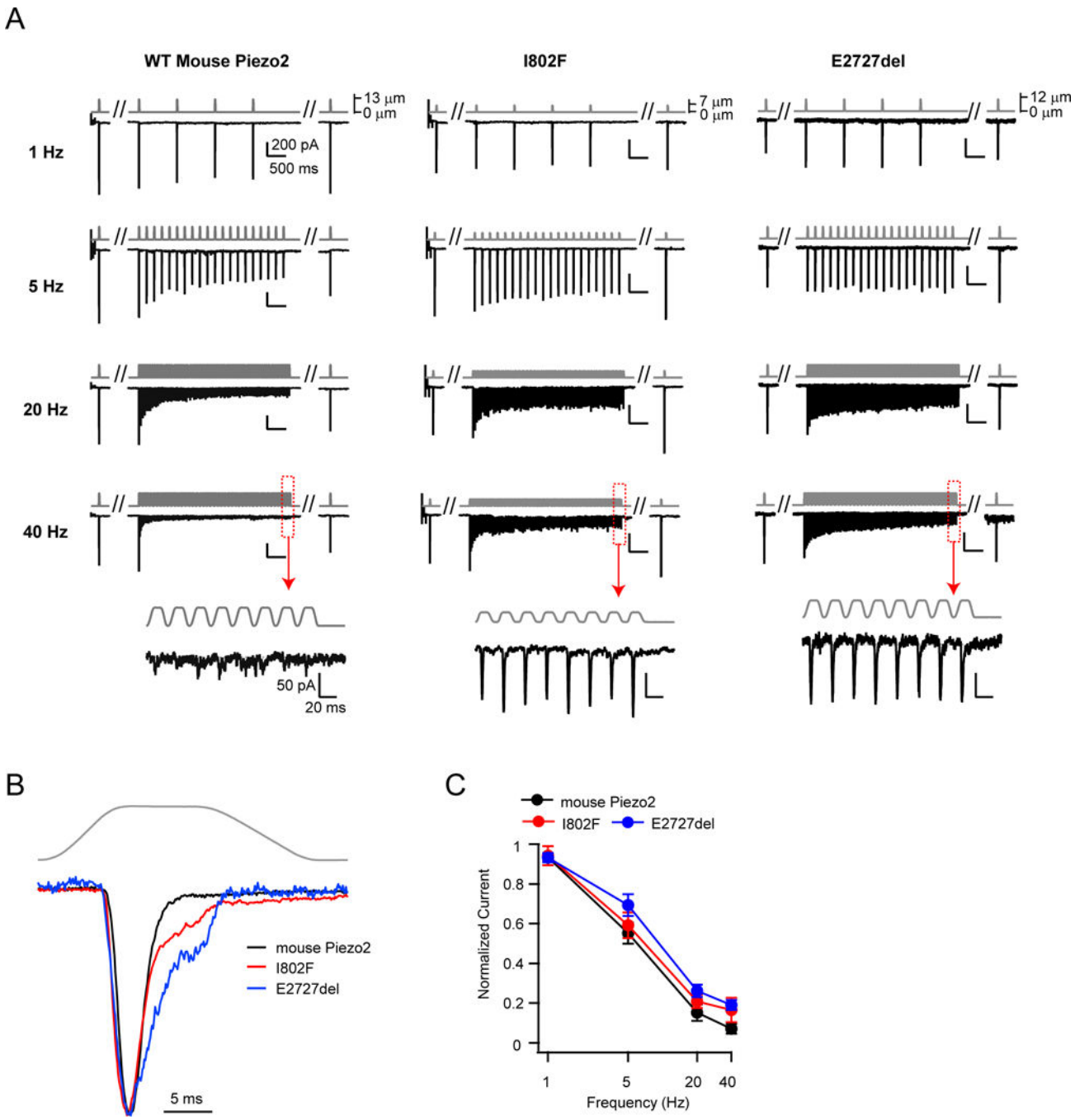

Figure 6. Piezo2 channels function as low-pass filters of square pulse poke stimuli

(A) Stimulus protocol (gray) and representative currents (black) from HEK293t cells transiently transfected with wild-type (left) or mutant Piezo2 (I802F, center and E2727del, right). Insets show responses to 40 Hz stimulation at an expanded timescale. (B) Representative currents of wild-type Piezo2 (black), and mutants I802F (red) and E2727del (blue) in response to a single test pulse. Currents are normalized to their peak. (C) Amplitude of the '*last peak*' current, normalized to the amplitude of '*first peak*' current at

each stimulation frequency. Holding potential was −100 mV. All data are mean ± s.e.m. N = 9–11 cells per construct.

Author Manuscript Author Manuscript Author Manuscript Author Manuscript

Author Manuscript Author Manuscript Author Manuscript Author Manuscript

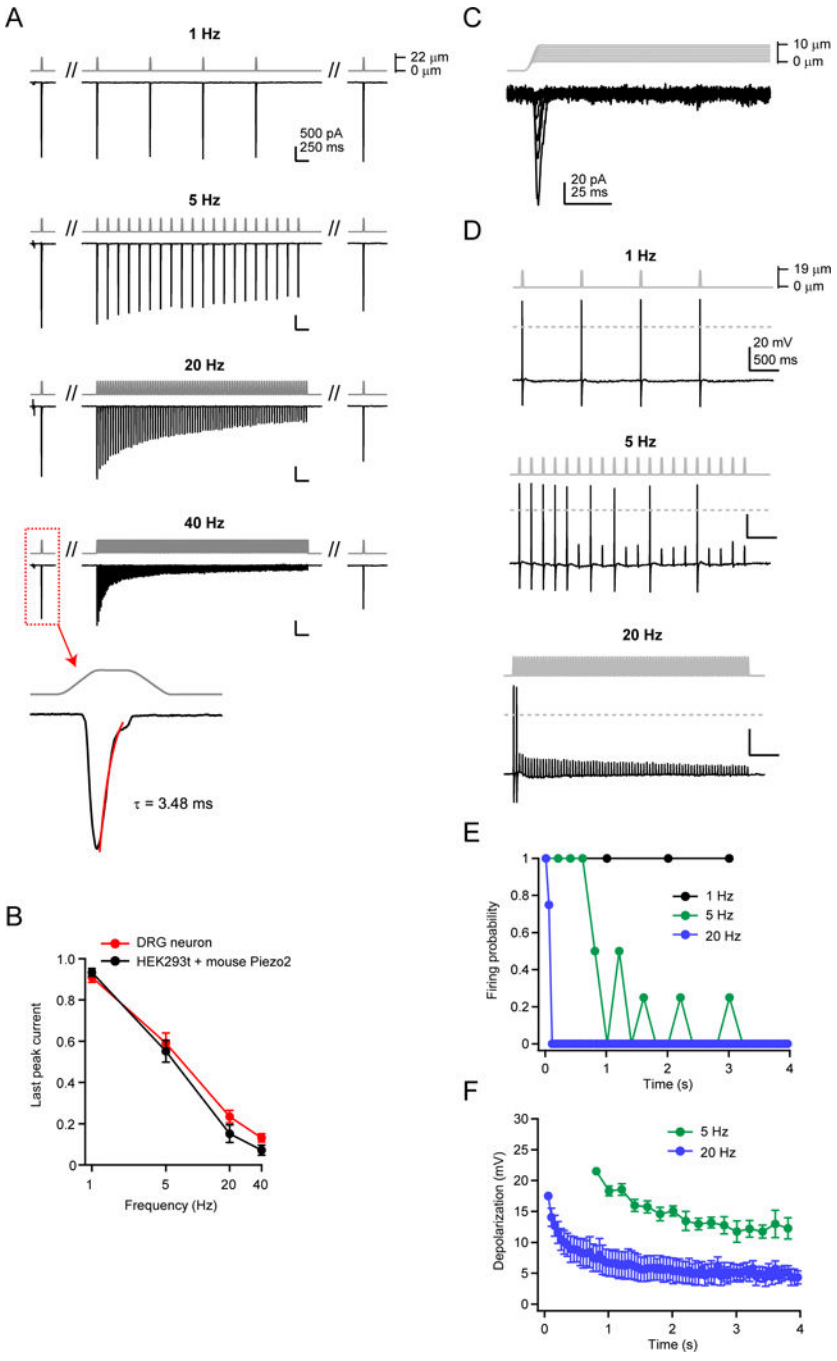

Author Manuscript Author Manuscript Author Manuscript Author Manuscript

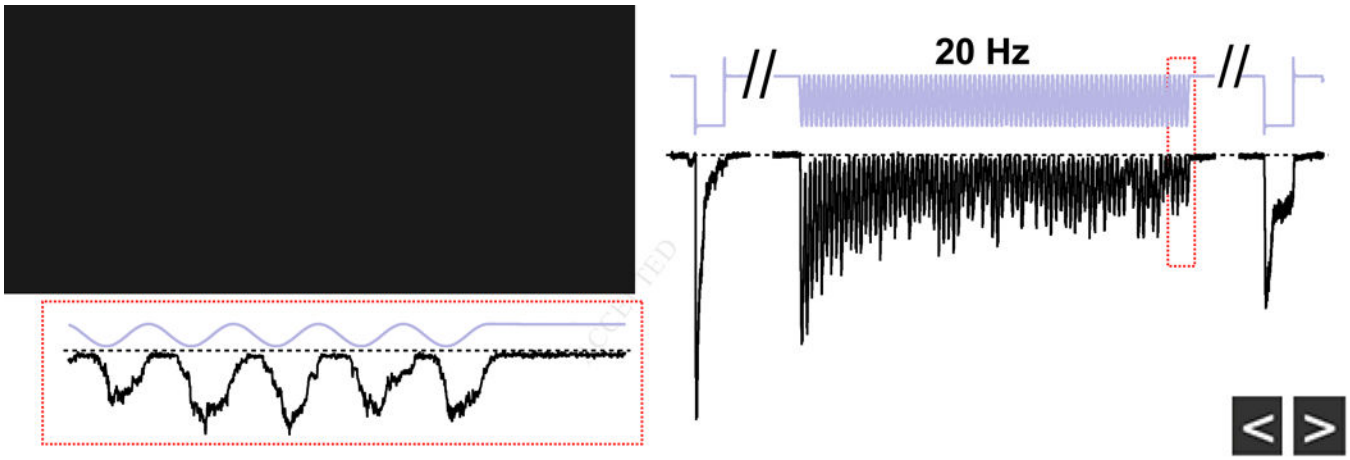

Figure 7. Rapidly-adapting DRG neurons show identical frequency filtering to mouse Piezo2 in HEK293t cells

(A) Stimulus protocol and representative currents from a whole-cell recording from a single mouse DRG neuron, elicited by a 20 ms square pulse poke stimulus at 1, 5, 20, and 40 Hz. All four frequencies were tested on the same cell. The cell displayed rapidly-adapting mechanosensitive currents (inset, 40 Hz), with an inactivation time course of τ <10 ms (Ranade et al., 2014b). Holding potential was −80 mV. (B) Amplitude of the last peak current, normalized to '*step1*', for rapidly-adapting DRG neurons (red, N = 7) and HEK293t cells transiently transfected with wild-type mouse Piezo2 (black, N = 10). (C) Stimulus protocol (gray) and representative current (black) from a rapidly-adapting DRG neuron in voltage clamp. (D) Stimulus protocol and action potentials elicited from the same neuron as in (C), in current clamp. Dashed line is 0 mV. (E) Firing probability for DRG neurons in response to 1, 5, and 20 Hz mechanical stimulation. Action potentials were counted for all responses crossing 0 mV. N = 4 neurons; all frequencies tested on each neuron. (F) Amplitude of subthreshold responses to 5 and 20 Hz from stimuli that failed to evoke action potentials in (E). All data are mean ± s.e.m.